resources

MDPI

Article

Olive Tree (*Olea europaea*) Pruning Autohydrolysis: FTIR Analysis, and Energy Potential

Idalina Domingos [1,*], Miguel Ferreira [2], José Ferreira [1] and Bruno Esteves [1]

[1] Centre for Natural Resources, Technology and Management School, Polytechnic University of Viseu, Av. Cor. José Maria Vale de Andrade, 3504-510 Viseu, Portugal; jvf@estgv.ipv.pt (J.F.); bruno@estgv.ipv.pt (B.E.)
[2] IT Department, Technology and Management School, Polytechnic University of Viseu, Av. Cor. José Maria Vale de Andrade, 3504-510 Viseu, Portugal; ferreira.miguel@estgv.ipv.pt
* Correspondence: ijd@estgv.ipv.pt

Abstract

Olive trees cultivated in the Viseu region (Portugal) were used in the present work. This study investigates the compositional characteristics and hydrothermal behavior of olive branches (OB) and olive leaves (OL) under autohydrolysis, aiming to assess their potential for biorefinery applications. Chemical analysis revealed that during autohydrolysis (140–180 °C, 15–30 min), OL exhibited greater solubilization than OB, consistent with their higher extractive content. Increasing the temperature promoted selective hemicellulose removal and partial cellulose degradation, leading to a relative enrichment of lignin in the solid residues. Nevertheless, the cellulose content of olive branches for 180 °C and 30 min hydrolysis increased. Fourier transform infrared spectroscopy confirmed progressive structural rearrangements, including enhanced hydroxyl exposure, carbonyl formation, and lignin condensation, indicating the transformation of the solid phase toward more aromatic and thermally stable structures. Autohydrolysis slightly increased the higher heating value of the solid residues while acid-catalyzed liquefaction markedly increased, exceeding those of both native and technical lignins. These results suggest extensive carbon enrichment and oxygen removal during liquefaction. Overall, autohydrolysis proved effective for hemicellulose solubilization and sugar recovery, while liquefaction favored energy densification and lignin condensation. The distinct behaviors of OB and OL highlight the importance of tailoring processing conditions to each feedstock type. Both materials show strong potential as renewable resources for bioenergy and value-added carbon-based products within an integrated olive biomass biorefinery framework.

Keywords: autohydrolysis; agro-industrial residues; chemical composition; FTIR; olive tree pruning

Received: 23 January 2026
Accepted: 6 February 2026
Published: 11 February 2026

1. Introduction

Olive trees, among the oldest cultivated species in human history, are now grown extensively across the globe, covering roughly 9 million hectares of agricultural land [1]. Reports from the International Olive Council (IOC) [2] rank Portugal as the sixth-largest olive oil producer globally, with a reported output of 150,000 tons during the 2023–2024 agricultural campaign, up from 126,000 tons in 2022–2023 [2]. This steady growth underscores the country's increasing prominence in the global olive oil sector. The expansion is largely driven by significant investments in super-intensive cultivation systems, modernization of milling infrastructure, and a strong commitment to high-quality production standards.

These advances have not only boosted production volume but have also enhanced the international reputation of Portuguese olive oils, particularly in export markets.

The rise in olive oil production in Portugal has also contributed to higher generation of olive by-products, especially olive leaves and small branches, which are produced in large quantities during pruning and oil extraction processes [1]. Olive trees in Portugal, as in other Mediterranean regions, require pruning annually or at least every two years [3], resulting in an average from each tree of around 25 kg of pruning residues, along with approximately 5% of the harvested olive weight as leaves collected at the mill [4]. Studies conducted in Mediterranean conditions indicate an average of 1.31 t/ha of pruning residues for annual pruning and 3.02 t/ha for biennial pruning [5], suggesting that similar values may be expected in Portuguese olive groves. Similarly, it is estimated that the production of one liter of olive oil generates about 6.23 kg of pruning residues, including branches and leaves [6]. Olive tree pruning has been stated to have around 25% woody fraction, another 25% leaves, and the remaining 50% thin branches [7].

The rich and diverse phenolic profile of olive leaves highlights their strong potential for valorization as high-value by-products within the agri-food, pharmaceutical, and nutraceutical sectors. According to Espeso et al. [1], olive leaves contain exceptionally high levels of bioactive compounds—particularly oleuropein, which can reach up to 24.5% of leaf dry weight—surpassing concentrations found in olive fruits and positioning leaves as a superior raw material for bioactive extraction [1,8,9]. The presence of other health-promoting phenolics, including hydroxytyrosol, verbascoside, flavones, flavonols, and phenolic acids, further enhances their functional value [1,10]. These compounds exhibit well-documented antioxidant, antimicrobial, and antiviral activities, making olive leaf extracts attractive for use as natural preservatives, functional food ingredients, cosmetic actives, or therapeutic agents [1,8,11]. Moreover, since olive leaves are generated in large quantities as agricultural residues during pruning and olive oil production, their exploitation supports circular economy principles by reducing waste and increasing resource efficiency. However, successful valorization depends on optimizing extraction technologies and carefully selecting raw materials, as polyphenolic composition is strongly influenced by agronomic conditions, leaf maturity, and processing parameters [1,8,12].

The extraction of these phenolic compounds from leaves also generates a residue since only the extractable compounds are removed, leaving the lignocellulosic fraction. The valorization of olive leaf waste after the extraction of phenolics was studied as a new source of fractions containing cellulose nanomaterials. The authors demonstrated that solid waste from extracted olive leaves could be efficiently valorized into different types of nanocellulose with distinct morphologies and properties, showing that lignin-containing nanocellulose offers higher yield, improved thermal stability, reduced hydrophilicity, and ultraviolet-absorbing capacity, while crystalline nanocellulose provides superior reinforcing performance in nanocomposite films [13]. Other examples showed that olive pruning has been successfully transformed into various cellulose-based materials, including pulp and paper sheets [14], microfibrillated cellulose [15], and nanocellulose, while cellulose isolated from pruning was converted into water-soluble hydroxypropyl carboxymethyl cellulose with short fibers and low mechanical strength [16].

Autohydrolysis, also referred to as water prehydrolysis, is a widely employed pretreatment technique in lignocellulosic biomass processing. In this method, biomass is treated with compressed hot water, which promotes the solubilization and depolymerization of hemicelluloses [17]. The process primarily generates sugars and oligosaccharides [18], facilitated by hydronium ions produced through the autoionization of water [19] and by organic acids released from the cleavage of acetyl groups. These acids act as catalysts, promoting the hydrolysis of glycosidic bonds and leading to the formation of lower molecular weight

polysaccharides, oligosaccharides, monosaccharides, and degradation products such as furfural and hydroxymethylfurfural. In addition to hemicellulose removal, autohydrolysis enhances the accessible surface area and decreases the crystallinity of cellulose, thereby improving its reactivity during subsequent enzymatic hydrolysis. However, excessive reaction time or high temperature can result in the conversion of xylose into furfural, reducing overall sugar yield; therefore, process parameters must be carefully optimized to balance sugar recovery and degradation [20]. Moreover, at elevated temperatures, partial lignin depolymerization can occur, releasing phenolic compounds into the hydrolysate [21].

The novelty of this work lies in the direct comparative assessment of olive leaves and olive branches processed under identical autohydrolysis conditions, integrating biochemical composition, structural analysis by infrared spectroscopy, and energy potential evaluation to clarify their differentiated roles within an olive-pruning-based biorefinery framework. This method offers a green, catalyst-free approach to biomass fractionation, enabling efficient separation with minimal environmental impact.

2. Materials and Methods

2.1. Material

Following the olive harvest in Viseu, a farm in central Portugal provided the olive tree pruning's for this study. These prunings consisted of leaves and thin branches, typically less than 2 cm in diameter.

The branches and leaves were separated, then milled using a Retsch SMI mill (Retsch, Haan, Germany) and subsequently sieved for 20 min at 50 rpm with a Retsch AS200 (Retsch, Haan, Germany). The 40 and 60 mesh (0.420–0.250 mm) fraction was dried in an oven at 105 °C for a minimum of 24 h and used for the tests.

2.2. Autohydrolisis

A Parr LKT PED cylindrical glass reactor (Parr Instrument Company, Moline, IL, USA) with a 600 mL capacity and double-walled insulation was used for the experiments. Inside the reactor, a 20 g sample of the 40–60 mesh fraction was combined with 200 mL of distilled water. An automatic stirrer maintained a consistent mixture at 70 rpm. The study focused on optimizing solubilization by varying the temperature (140, 160, and 180 °C) and reaction time (15 and 30 min at each temperature). These temperatures and times have been chosen in order to have means of comparison against the liquefaction procedure [22]. The tests were made in duplicate. Approximately 10 min were required for the reactor's internal temperature to reach the set point. After each test, the mixture was filtered through a Buchner funnel with filter paper to separate the solid residue from the liquid. The solid residue was then dried in an oven at 103 ± 2 °C and weighed to determine the percentage of solubilized material, as described in Equation (1).

$$Solubilization(\%) = \frac{Initial\ dry\ mass(\mathrm{g}) - Solid\ dry\ residue\ (\mathrm{g})}{Initial\ dry\ mass\ (\mathrm{g})} \times 100 \quad (1)$$

2.3. Chemical Composition of Solid Residues After Autohydrolisis

Lignin in extractive-free olive branches and leaves was quantified using a modified Klason method, involving two hydrolysis steps (72% H_2SO_4 at 30 °C for 1 h, followed by 3% H_2SO_4 in an autoclave at 1.2 bar for 1 h) [23]. Holocellulose was measured via the acid-chlorite method to remove nearly all lignin, and α-cellulose content was determined for extractive-free samples according to TAPPI 429 cm-23 [24]; hemicellulose was determined as the difference between holocellulose and α-cellulose.

2.4. Infrared Spectroscopy Analysis

FTIR-ATR spectroscopy was used to characterize the initial dried material and the solid residue after autohydrolysis. A Perkin Elmer UATR Spectrum Two (Perkin Elmer, Bridgeport, CT, USA) spectrometer was used, collecting 72 scans per minute with a resolution of 4.0 cm^{-1} over the 4000 to 400 cm^{-1} range. Samples were dried at 103 ± 2 °C for one week beforehand to ensure complete moisture removal. A background spectrum was acquired by measuring the absorbance over the crystal. Solid samples were then placed and pressed firmly onto the crystal, covering its entire surface. An average of three spectra were collected for each sample. No mathematical post-treatment or band normalization was applied, as ATR-FTIR allows direct qualitative and semi-quantitative comparison of spectra when acquisition parameters and sample–crystal contact conditions are kept constant.

2.5. Liquefaction

Liquefaction of dried olive branch and leaf powders was carried out in a glycerol–ethylene glycol solvent with sulfuric acid as a catalyst under controlled temperature and stirring, followed by cooling, methanol dissolution and filtration as described before [22].

2.6. Heating Value

The sample used in the determination of the calorific value (high heating value) was grounded after being completely dried at 105 °C, and subsequently, it was subjected to compression (4 ton, 10 s) to produce a 1 cm diameter pellet, which was inserted into the heat pump. Three replicates of each sample were made. A Parr calorimeter-model 6400 was employed for this evaluation. Since it is not possible to quantify directly the heat released during the combustion, the temperature rises in the water contained in the calorimetric container surrounding the sample is measured. Knowing the temperature rise and the calorific capacity of water, the HHV of the sample was obtained.

3. Results and Discussion

The chemical composition of olive branches (OB) and olive leaves (OL) presented before shows that olive leaves have higher ash (4.08%) and extractive contents, 5.80% (dichloromethane), 20.11% (ethanol), and 15.82% (hot water) compared with branches with 2.79% and 1.22%, 11.24%, and 10.00% respectively. On the other end, olive branches contained higher levels of structural carbohydrates, with 30.47% α-cellulose and 27.88% hemicellulose, against 18.56% and 14.00% for leaves along with a lower Klason lignin content (16.40%) compared to leaves (21.64%) [22]. This compositional distinction is particularly relevant for the olive oil industry, as olive leaves are generated in large quantities during harvesting and cleaning operations, and their higher extractive content suggests a greater potential for recovering value-added compounds alongside olive oil production. Olive leaves are particularly rich in phenolic extractives, dominated by oleuropein and accompanied by significant amounts of hydroxytyrosol, verbascoside, flavones, flavonols, and phenolic acids, which can be extracted leaving the lignocellulosic fraction for further processing [1,8,9].

The solubilization behavior of olive biomass under autohydrolysis (Figure 1) varies markedly between olive branches and olive leaves, with both temperature and reaction time significantly influencing the extent of solubilization. In general, olive leaves (OL), which have higher contents of extractives such as ethanol-soluble and hot water-soluble compounds, exhibited higher solubilization percentages than olive branches across all tested conditions. From an olive oil industry perspective, this behavior highlights the suitability of olive leaves for mild hydrothermal processing steps that could be integrated downstream of oil extraction, enabling the recovery of soluble fractions without extensive

preprocessing. At 140 °C, solubilization of olive leaves reached 31.41% after 15 min and slightly increased to 32.79% at 30 min, while olive branches showed significantly lower values of 18.97% and 20.28%, respectively. This higher solubilization in leaves for lower temperatures and times is likely due to their higher extractive content (41.73%) compared to branches (22.46%). At 160 °C, the trend continued but with smaller differences, with solubilization increasing for both materials. Olive leaves reached 36.11% after 30 min, while olive branches reached 27.24%, suggesting that moderate temperature and prolonged treatment promote the partial breakdown of hemicellulosic and extractive fractions. At 180 °C, both olive leaves and olive branches maintained their upward trend, with solubilization rising from 40.51% (15 min) to 45.16% (30 min) for OL and olive branches from 30.26% (15 min) to 36.37% (30 min). These results highlight how the higher proportion of extractives in OL facilitate more efficient solubilization during autohydrolysis.

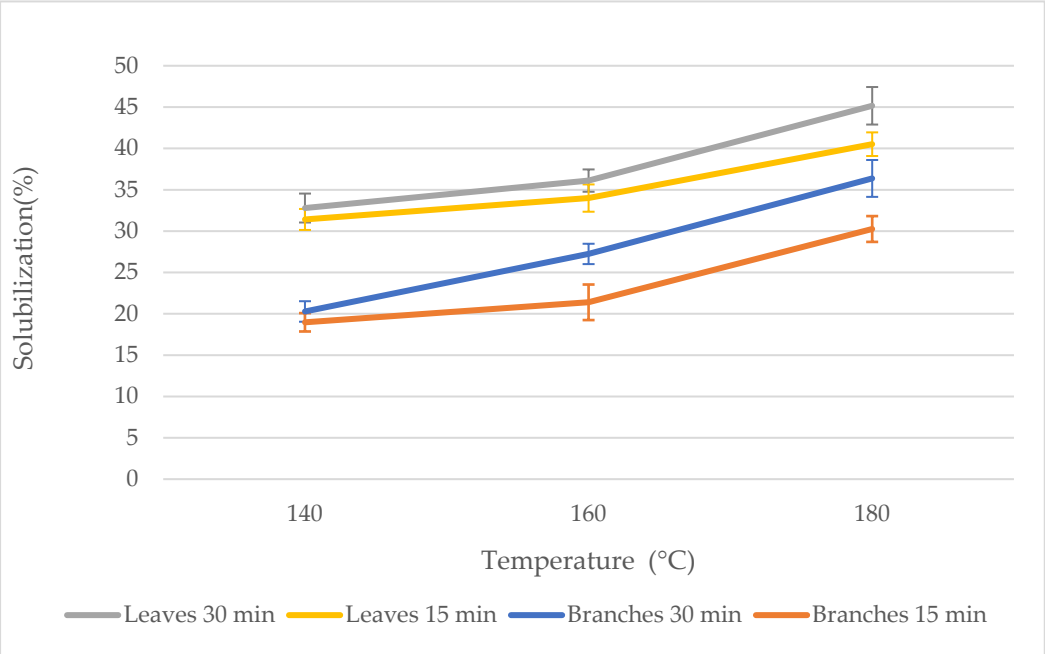

Figure 1. Solubilization percentage due to autohydrolysis of olive leaves (OL) and branches (OB).

The autohydrolysis of several other lignocellulosic materials leads to similar solubilizations. For instance, sweet cherry seeds showed a 26.7% solubilization obtained at 170 °C and 180 min [25] while Romaní et al. [26] reported a solid residue varying from 18.2 to 27.6% for the autohydrolysis of *Eucalyptus globulus* with severity factors ranging from 3.35 to 3.94. The comparable behavior of olive residues confirms that by-products of the olive oil industry can be processed using established hydrothermal technologies already validated for other agro-industrial sectors.

Figures 2 and 3 present the macromolecular chemical composition of the solid residue after the autohydrolysis of olive leaves and olive branches at 140 °C, 160 °C and 180 °C for 15 and 30 min, respectively. The chemical composition of the solid residues obtained from the autohydrolysis of olive leaves and olive branches reveals significant trends influenced by both temperature (140–180 °C) and reaction time (15 and 30 min). The major components analyzed, lignin, α-cellulose, and hemicellulose, undergo distinct transformations, reflecting typical patterns of lignocellulosic fractionation under hydrothermal conditions. Lignin content increased steadily with rising temperature in all samples. Nevertheless, this apparent increase does not necessarily reflect lignin condensation or polymerization but is largely attributed to the preferential solubilization of hemicelluloses and, to a lesser extent, cellulose, leading to a relative enrichment of lignin in the solid residue [27]. For olive oil

producers, this lignin enrichment is particularly relevant as it enhances the suitability of the remaining solid for energy recovery or advanced material applications, potentially offsetting processing costs.

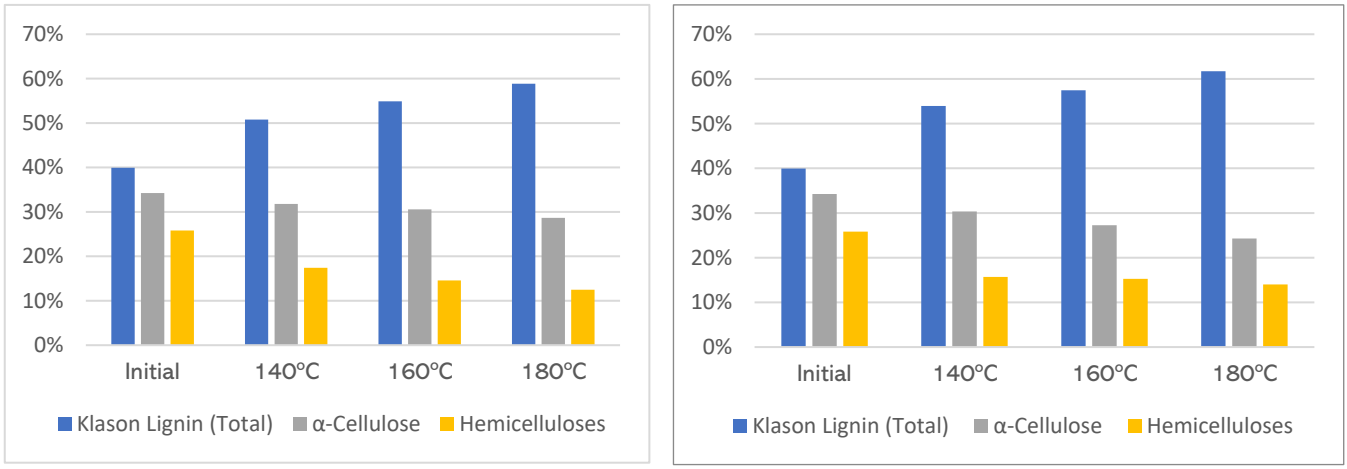

Figure 2. Chemical composition of olive leaves (OL) after autohydrolysis for 15 (**left**) and 30 (**right**) min.

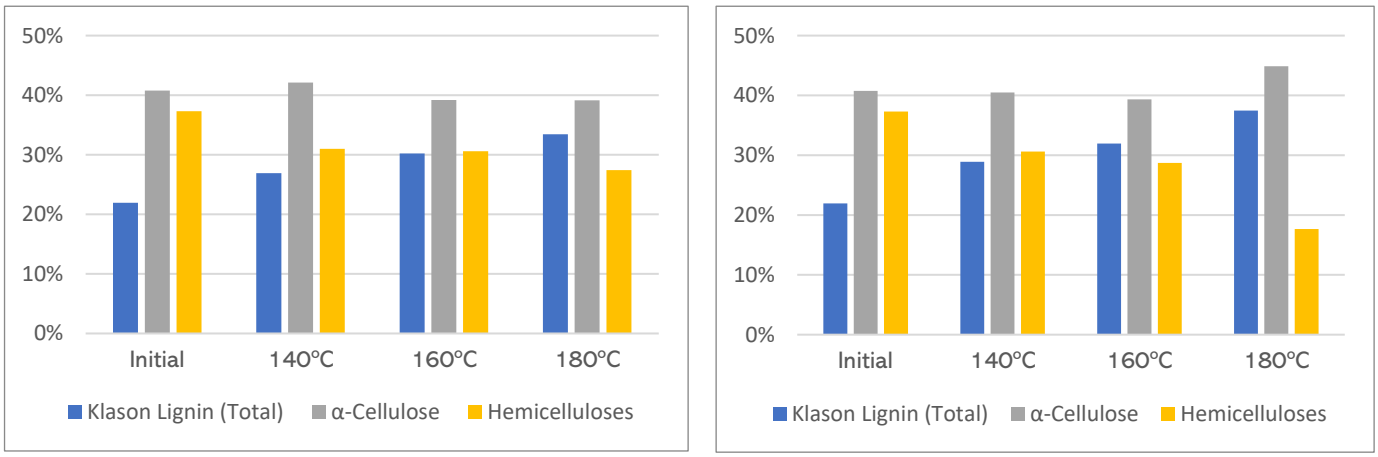

Figure 3. Chemical composition of olive branches (OB) after autohydrolysis for 15 (**left**) and 30 (**right**) min.

For OL at 15 min, lignin content rose from the initial 39.92% to 50.79% at 140 °C reaching 58.84% at 180 °C. A similar trend was observed for 30 min, with lignin increasing to 53.96% and 61.72% at 140 °C and 180 °C, respectively. In OB, the lignin content also increased from the initial content (21.93%) to 26.90% at 140 °C and 33.45% at 180 °C for 15 min and to 28.90% and 37.47% at 30 min for 140 °C and 180 °C, respectively. The overall higher lignin content in OL compared to OB highlights the intrinsic compositional differences between leaves and woody biomass as seen before [22]. This distinction suggests that olive leaves may be more suitable for phenolic-rich extracts and antioxidant recovery, whereas branches may be better aligned with structural or energy-oriented valorization routes within olive oil supply chains. Similar results have been reported before for different wood as, for example, for the autohydrolysis of *Eucalyptus globulus* wood at 160 °C and 30–66 min where Klason lignin increased from 23.1% to 29.4% while xylan and arabinan decreased to almost half of the initial content [28]. Romaní et al. [26], also for the autohydrolysis of eucalypt wood, reported an increase from 26.3 to 32.0%. Comparable trends were observed for *Pinus radiata* treated at 150–190 °C for 30–90 min, where lignin content rose with

increasing temperature and reaction time [29], and for Scots pine sapwood processed at temperatures between 130 °C and 170 °C [30]. Similar corroborating results were presented for other lignocellulosic materials such as sweet cherry seeds [25] or hazelnut shells [27] where Klason lignin increased from 38.1% to 44.9% and 36.7% to 52.6% respectively or for pine nut shells [31].

Even though there is an increase in lignin percentage, studies have shown that lignin also changes along autohydrolysis. Studies show that as the duration of autohydrolysis increases, lignin fractions have a reduction in aliphatic hydroxyl group content and β–O–4 linkages, while the proportion of phenolic hydroxyl groups increases [32]. Similar results were presented by Jia et al. [33] who found out that with the increasing hydrolysis intensity of wood chips, the β-O-4 linkages in lignin decreased by 57.1%, whereas the β-5 and β-β linkages and the S/G ratio increased by 66.7%, 41.8%, and 151%, respectively. Additionally, these authors stated that the phenolic OH content of lignin increased, while the aliphatic OH groups decreased with higher autohydrolysis severity.

The α-cellulose content in OL decreased slightly with temperature: from 34.24% to 31.79% (140 °C) and 28.66% (180 °C) at 15 min, and to 30.33% (140 °C) to 24.28% (180 °C) at 30 min. In OB α-cellulose is approximately constant at around 40% for autohydrolysis for 15 min with an increase at 180 °C for 30 min (44.88%), indicating greater thermal and hydrolytic stability of OB cellulose under these conditions. This suggests that olive leaves may contain a more amorphous or less crystalline form of cellulose, making it more susceptible to hydrothermal degradation compared to the more lignified and structured olive branches. On the other hand, it can also be due to the higher degradation of hemicelluloses observed in olive branches. The preferential degradation of amorphous cellulose has been reported before. For instance, following autohydrolysis, the crystallinity index of the milled *E. pellita* rose from 59.7% to 69.6%. The increase results from the selective removal of the hemicellulose fraction, which diminishes the amorphous components of the biomass and enhances overall crystallinity [34].

Most of the reported results state that cellulose is maintained in the solid residue. For example, in accordance with Romaní et al. [26] the contents of cellulose ranged from 54.3 to 61.4%, indicating that cellulose was almost quantitatively retained in the solid fraction. Similarly, Yang et al. [35] reported that glucan content remained relatively stable or slightly increased along the autohydrolysis of poplar chips while Lobato-Rodríguez et al. [36] reported a slight reduction (1.87% at the highest severity) for the autohydrolysis of *Acacia dealbata*.

In relation to hemicelluloses, as expected, they showed the most pronounced decrease across all temperatures and times. In OL (30 min), the initial 25.83% content declined, reaching 15.70% at 140 °C and 14.00% at 180 °C and similarly for 15 min samples. For OB, the decrease was to 30.99% and 27.42% at 15 min and 30.61% to 17.65% at 30 min (Figure 2), indicating more substantial hemicellulose presence in OB but also higher susceptibility to solubilization, especially at 30 min. These reductions are consistent with the greater reactivity and lower thermal stability of hemicelluloses, particularly under autohydrolysis where acetic acid released from acetyl groups acts as a catalyst for depolymerization [27].

The results show that increasing the severity of autohydrolysis (by raising temperature and extending reaction time) led to a gradual decrease in solid yield and xylan content. Similar results were reported for poplar wood chips, where xylan content was reported to declined markedly—from 17.31% in the control to 11.30% at the highest severity—reflecting the selective removal of hemicelluloses [35]. Also, Lobato-Rodríguez et al. [36] stated that the analysis of *Acacia Dealbata* residue after autohydrolysis revealed that hemicellulose solubilization, expressed as the combined release of xylan, arabinan, and acetyl groups, increased markedly from 71.26% to 92.36% as treatment severity rose from 3.63 to 4.64.

The same was reported for *Robinia pseudoacacia* wood where hemicellulose solubilization increased with rising temperature and residence time [37]. These authors stated that at 200 °C, extending the reaction time from 0 to 30 min enhanced hemicellulose solubilization from 12% to 85% of the initial content.

The solubilization percentage obtained during autohydrolysis exhibited a clear correlation with the chemical composition of the resulting solid residues, reflecting the progressive fractionation of the olive biomass components. As solubilization increased with temperature and reaction time, a concomitant decline in hemicellulose content was observed in both olive leaves (OL) and olive branches (OB), confirming that hemicelluloses are the most hydrolytically labile polymers under hydrothermal conditions. The enhanced solubilization at higher severities led to a relative enrichment of lignin in the solid residues, not due to additional lignin formation, but rather due to the preferential dissolution of hemicelluloses and partial removal of amorphous cellulose [27]. This effect was particularly pronounced in OL, where higher initial extractive content facilitated greater solubilization and consequently a more significant apparent increase in lignin proportion (up to 61.72% at 180 °C, 30 min). In contrast, OB, characterized by a more crystalline cellulose structure and lower extractive content, exhibited lower solubilization values and a relatively stable cellulose fraction, suggesting higher resistance to hydrothermal degradation. The decline in hemicellulose content, coupled with moderate cellulose loss, indicates that the solubilization process selectively targets the more amorphous and less ordered carbohydrate domains. Thus, higher solubilization percentages correspond to solids enriched with lignin and cellulose, with reduced hemicellulose fractions, demonstrating that process severity governs the chemical redistribution between the liquid and solid phases. This relationship underscores the need to optimize temperature and residence time to balance hemicellulose removal and cellulose preservation, particularly when designing autohydrolysis conditions for integrated biorefinery applications.

Figures 4 and 5 present the FTIR spectra of initial olive leaf and olive branch material and the solid residues obtained after 30 min autohydrolysis at different temperatures and at 180 °C and at different times. Overall, the spectral profiles indicate progressive structural modifications of the main biopolymeric constituents, particularly carbohydrates and lignin. One of the first observable changes occurs in the broad O–H stretching region around 3400 cm^{-1} [38]. While the initial material shows a single broad absorption typical of strongly hydrogen-bonded hydroxyl groups in cellulose, hemicellulose and phenolic structures, the treated samples exhibit the emergence of a distinct shoulder at approximately 3470 cm^{-1}. The appearance of this shoulder suggests the formation or exposure of hydroxyl groups that are less strongly hydrogen-bonded. This modification can be attributed to the hydrolytic cleavage of glycosidic bonds within hemicellulose and amorphous cellulose domains, which generates new terminal hydroxyl functionalities. In addition, partial depolymerization of lignin may release phenolic hydroxyl groups, which also absorb at higher wavenumbers when they participate in weaker hydrogen bonding. The shoulder therefore reflects an increase in free or weakly associated hydroxyl groups, indicating that the structure of the solid residue becomes more fragmented and chemically accessible as the solubilization temperature increases.

In the aliphatic C–H stretching region, where the peaks are at 2915 cm^{-1} and 2850 cm^{-1}, corresponding to asymmetric and symmetric vibrations [39,40], progressive temperature increase leads to a noticeable enhancement at 2920 cm^{-1}, which shifts slightly toward 2930 cm^{-1}, along with a clear increase in the 2850 cm^{-1} band and the appearance of a shoulder at approximately 2867 cm^{-1}. These observations suggest a reorganization or enrichment of aliphatic structures in the solid phase. This may reflect either the partial removal of polysaccharides, leading to a relative concentration of lignin and lipid-derived

moieties, or thermal rearrangement within the remaining cell wall matrix. This is in accordance with the chemical composition of the solid residues in Figures 2 and 3.

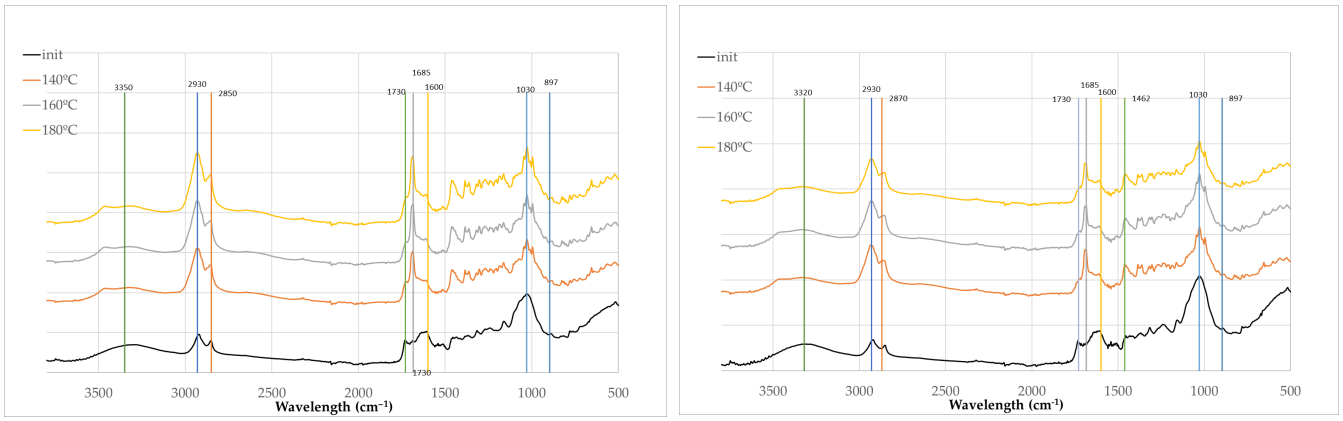

Figure 4. FTIR spectra of initial olive leaf material (**left**)/olive branches (**right**) and the solid residues obtained after 30 min autohydrolysis at different temperatures.

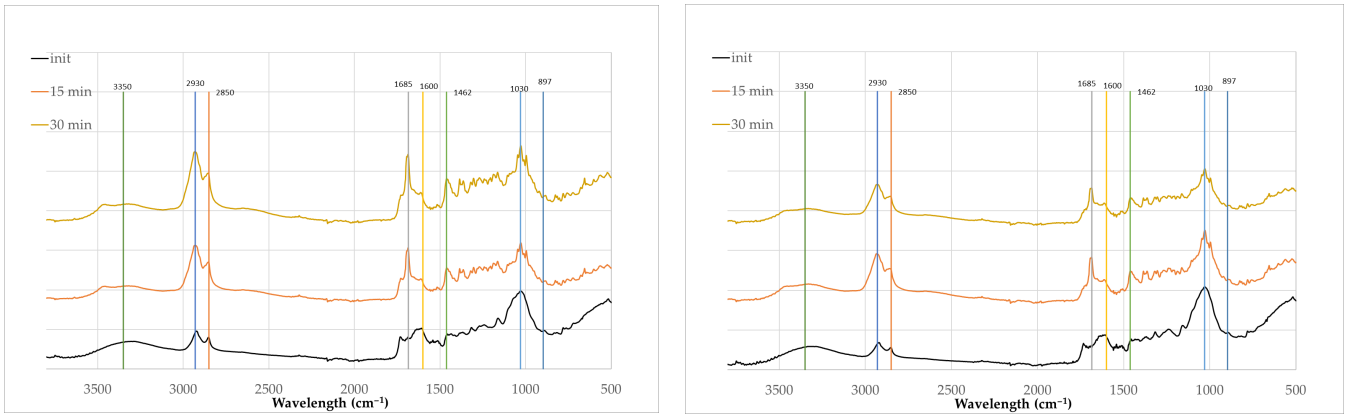

Figure 5. FTIR spectra of initial olive leaf material (**left**)/olive branch (**right**) material and the solid residues obtained at 180 °C autohydrolysis at different times.

A significant decrease in the 1730 cm^{-1} peak attributed to C=O stretching vibration of acetyl ester groups in hemicelluloses [39,40] was observed with autohydrolysis which confirms the chemical composition presented in Figures 2 and 3. Similarly, Paulownia wood autohydrolysis leads to the near-complete disappearance of the 1731 cm^{-1} peak in the solid residue [41]. Equally, the autohydrolysis of vine shoot presented the same result [42].

Substantial changes also occur in the carbonyl and aromatic region. A strong peak emerges at 1685 cm^{-1} and intensifies with temperature, indicating the formation of conjugated carbonyl groups [39], likely arising from oxidative or dehydration reactions during treatment. At the same time, the band near 1600 cm^{-1} decreases slightly in intensity which could reflect some changes in lignin structure. Different results were presented before for the hydrolysis of hazelnut shells where the 1600 cm^{-1} peak increased with the development of the hydrolysis [27].

The peak at 1462 cm^{-1} becomes more pronounced with the hydrolysis, since this peak indicates CH_2 (and sometimes CH_3) bending vibrations [39] associated with cellulose and lignin structures; this can be due to the increase in these compounds in the solid residue as determined before.

In the fingerprint region, the carbohydrate-associated peaks at 1044, 1030, and 995 cm^{-1} become more sharply defined in the samples treated at higher temperatures. The

improved resolution of these bands suggests a change in the molecular environment of the polysaccharide framework, potentially due to the removal of amorphous hemicellulose fractions and the increased ordering or exposure of cellulose microdomains that remain in the solid residue.

Overall, the evolution of the spectra indicates that increasing treatment temperature promotes the hydrolysis of amorphous carbohydrate components and induces structural rearrangements in lignin and aliphatic constituents. The residues thus become enriched in lignin- and lipid-related structures while also displaying a higher density of newly accessible hydroxyl groups. These chemical and structural transformations are expected to influence both the reactivity and the functional performance of the resulting solid material in subsequent valorization or application steps. The results presented before for the FTIR spectra of poplar wood lignin following autohydrolysis at several severity factors showed that there were no significant changes in lignin structure [35].

The changes observed with the increase in autohydrolysis temperature (Figure 4) are similar to those obtained at different autohydrolysis times (Figure 5). The main difference between the solid residue of olive leaves and olive branches is the higher intensity of the 1685 cm^{-1} peak in olive leaves and somewhat at 2930 cm^{-1} and 2850 cm^{-1}.

The changes in the high heating value (HHV) of olive leaves and branches with autohydrolysis were determined and compared with acid-catalyzed polyalcohol liquefaction at similar conditions and are presented in Table 1. Since both autohydrolysis and acid-catalyzed liquefaction lead to an enrichment in lignin content, it is expected that the HHV of the solid residues increase due to the higher HHV of lignin compared to those of polysaccharides. Autohydrolysis, however, increased the energy content of olive branches and leaves far less than that of acid-catalyzed liquefaction, which produced a substantially higher enhancement. When branches were liquefied at 180 °C for 30 min, their solid residue reached an HHV of 30.39 MJ/kg (±0.40), whereas the autohydrolyzed branches had only reached 19.45 MJ/kg (±0.09). Even after just 15 min of liquefaction, the branches' HHV (28.54 MJ/kg) exceeded that of the 15 min autohydrolyzed material (19.42 MJ/kg) by almost half. Leaves showed the same trend. Liquefaction for 30 min produced a residue with an HHV of 29.31 MJ/kg (±0.55), compared with 23.92 MJ/kg (±0.39) from autohydrolysis. A 15 min treatment under liquefaction still outperformed water alone, yielding 28.04 MJ/kg versus 23.53 MJ/kg for autohydrolyzed leaves. Extending the reaction time from 15 to 30 min during liquefaction raised the HHV by roughly 6 percent for branches and 4.5 percent for leaves, suggesting that longer exposure to the acid-catalyzed polyalcohol environment continued to enhance the residue's energy density. In contrast, the autohydrolysis method showed negligible change in HHV with time: the branches' heating value varied by less than 0.2 percent and the leaves' by under 1.7 percent between 15 and 30 min, which could imply that most of the soluble hemicellulose had already been removed within the shorter period.

Table 1. HHV of the solid residues after liquefaction and autohydrolysis of olive branches and olive leaves.

			Liquefaction		**Autohydrolysis**	
Olive Tree	**Temp. (°C)**	**Time (Min)**	**HHV (MJ/kg)**	**Std. Dev.**	**HHV (MJ/kg)**	**Std. Dev.**
Branches	180 °C	30′	30.3874	0.4031	19.4491	0.0861
Branches	180 °C	15′	28.5416	0.2158	19.4173	0.0465
Leaves	180 °C	30′	29.3103	0.5539	23.9154	0.3864
Leaves	180 °C	15′	28.0355	0.9280	23.5332	0.2003

The difference between branches and leaves also narrowed under liquefaction. Where autohydrolyzed leaves consistently produced a higher HHV (around 23.5–23.9 MJ/kg) than branches (19.4 MJ/kg), the polyalcohol liquefaction left a residue whose HHV approached that of low-rank coals for both materials—30.4 MJ/kg for branches and 29.3 MJ/kg for leaves after 30 min.

Results on the HHV of liquefied branches and leaves suggests that the residue is mainly constituted of highly condensed lignin due to an increased proportion of condensed aromatic structures since the HHV is over 28 MJ/kg, which is notably higher than the typical range reported for both native and technical lignins. For instance, lignins isolated using sulfur-based methods from softwoods such as spruce and pine yielded HHVs of 26.73 MJ/kg and 27.00 MJ/kg, respectively, while hardwood lignin from poplar showed a lower value of 25.45 MJ/kg. Similarly, herbaceous materials like bagasse, switchgrass, straw, and corn stalks all exhibited HHVs of around 25.2 MJ/kg [43,44]. The value for spruce lignin was also close to the estimated HHV for native lignin (26.85 MJ/kg) [44,45].

Technical lignins derived from industrial processes present more variability but also lower values like, for instance, UPM BioPiva™ 100 and 300 demonstrated HHVs of 26.9 MJ/kg and 27.1 MJ/kg, respectively [46].

4. Conclusions

The comparative evaluation of olive branches (OB) and olive leaves (OL) under autohydrolysis reveals distinct compositional and reactivity behaviors linked to their intrinsic structures. Olive leaves, with higher extractive and ash contents and lower structural carbohydrates, showed greater solubilization during autohydrolysis, while olive branches, richer in cellulose and hemicellulose, exhibited higher structural stability and lower solubilization. Autohydrolysis primarily removed hemicelluloses and partially degraded amorphous cellulose, resulting in lignin-enriched residues, with temperature being the dominant factor and reaction time further enhancing polysaccharide solubilization. FTIR analyses indicated progressive molecular rearrangements, including increased hydroxyl exposure, the formation of carbonyl groups, and the enrichment of aromatic structures at higher severities.

Autohydrolysis slightly increased the energy content of both biomasses but to a lesser extent than in acid-catalyzed polyalcohol liquefaction. Overall, both olive residues are promising biorefinery feedstocks, with autohydrolysis favoring hemicellulose recovery and showing to be an efficient first fractionation step within a biorefinery framework for olive oil industry residues.

Overall, this work provides a coherent framework for aligning olive biomass composition with targeted conversion pathways, enabling the more efficient, sustainable, and value-driven integration of olive residues into advanced biorefinery systems.

Author Contributions: Conceptualization, I.D. and J.F.; methodology, I.D. and B.E.; software, M.F.; validation, B.E.; formal analysis, I.D. and B.E.; investigation, I.D., M.F. and B.E.; resources, I.D. and J.F.; data curation, I.D., M.F. and B.E.; writing—original draft preparation, I.D. and B.E.; writing—review and editing, I.D., M.F., J.F. and B.E.; supervision, B.E.; funding acquisition, I.D. and J.F. All authors have read and agreed to the published version of the manuscript.

Funding: This work was funded by National Funds through the FCT—Foundation for Science and Technology, I.P.—within the scope of the project Ref[a] UID/00681/2025, https://doi.org/10.54499/UID/00681/2025.

Data Availability Statement: The original contributions presented in this study are included in the article. Further inquiries can be directed to the corresponding author.

Acknowledgments: We would like to thank the CERNAS Centre and the Polytechnic University of Viseu for their support.

Conflicts of Interest: The authors declare no conflicts of interest.

References

1. Espeso, J.; Isaza, A.; Lee, J.Y.; Sörensen, P.M.; Jurado, P.; Avena-Bustillos, R.D.J.; Olaizola, M.; Arboleya, J.C. Olive Leaf Waste Management. *Front. Sustain. Food Syst.* **2021**, *5*, 660582. [CrossRef]
2. International Olive Council. Available online: https://www.internationaloliveoil.org/wp-content/uploads/2023/12/HO-CE901-13-12-2023-P.pdf (accessed on 22 April 2025).
3. Bruno, M.R. Variability and Chemical Composition of the Extractive Content of Woody Residues from Three European Orchard Species: Apricot (*Prunus armeniaca* L.), Olive (*Olea europea* L.), and Orange Trees (*Citrus sinensis* L.). *JSFA Rep.* **2023**, *3*, 82–97. [CrossRef]
4. Ramírez, E.M.; Brenes, M.; Romero, C.; Medina, E. Chemical and Enzymatic Characterization of Leaves from Spanish Table Olive Cultivars. *Foods* **2022**, *11*, 3879. [CrossRef]
5. Velázquez-Martí, B.; Fernández-González, E.; López-Cortés, I.; Salazar-Hernández, D.M. Quantification of the Residual Biomass Obtained from Pruning of Trees in Mediterranean Olive Groves. *Biomass Bioenergy* **2011**, *35*, 3208–3217. [CrossRef]
6. Avraamides, M.; Fatta, D. Resource Consumption and Emissions from Olive Oil Production: A Life Cycle Inventory Case Study in Cyprus. *J. Clean. Prod.* **2008**, *16*, 809–821. [CrossRef]
7. Selim, S.; Albqmi, M.; Al-Sanea, M.M.; Alnusaire, T.S.; Almuhayawi, M.S.; AbdElgawad, H.; Al Jaouni, S.K.; Elkelish, A.; Hussein, S.; Warrad, M.; et al. Valorizing the Usage of Olive Leaves, Bioactive Compounds, Biological Activities, and Food Applications: A Comprehensive Review. *Front. Nutr.* **2022**, *9*, 1008349. [CrossRef]
8. Benavente-García, O.; Castillo, J.; Lorente, J.; Ortuño, A.; Del Rio, J.A. Antioxidant Activity of Phenolics Extracted from *Olea europaea* L. Leaves. *Food Chem.* **2000**, *68*, 457–462. [CrossRef]
9. Herrero, M.; Temirzoda, T.N.; Segura-Carretero, A.; Quirantes, R.; Plaza, M.; Ibañez, E. New Possibilities for the Valorization of Olive Oil By-Products. *J. Chromatogr. A* **2011**, *1218*, 7511–7520. [CrossRef]
10. Khelouf, I.; Karoui, I.J.; Lakoud, A.; Hammami, M.; Abderrabba, M. Comparative Chemical Composition and Antioxidant Activity of Olive Leaves *Olea europaea* L. of Tunisian and Algerian Varieties. *Heliyon* **2023**, *9*, e22217. [CrossRef]
11. Andrikopoulos, N.K.; Kaliora, A.C.; Assimopoulou, A.N.; Papageorgiou, V.P. Inhibitory Activity of minor Polyphenolic and Nonpolyphenolic Constituents of Olive Oil Against In Vitro Low-Density Lipoprotein Oxidation. *J. Med. Food* **2002**, *5*, 1–7. [CrossRef] [PubMed]
12. Şahin, S.; Bilgin, M. Olive Tree (*Olea europaea* L.) Leaf as a Waste by-Product of Table Olive and Olive Oil Industry: A Review. *J. Sci. Food Agric.* **2018**, *98*, 1271–1279. [CrossRef] [PubMed]
13. Ben Mabrouk, A.; Putaux, J.-L.; Boufi, S. Valorization of Olive Leaf Waste as a New Source of Fractions Containing Cellulose Nanomaterials. *Ind. Crops Prod.* **2023**, *202*, 116996. [CrossRef]
14. Díaz, M.J.; Eugenio, M.E.; López, F.; Alaejos, J. Paper from Olive Tree Residues. *Ind. Crops Prod.* **2005**, *21*, 211–221. [CrossRef]
15. Ibarra, D.; Martín-Sampedro, R.; Wicklein, B.; Fillat, Ú.; Eugenio, M.E. Production of Microfibrillated Cellulose from Fast-Growing Poplar and Olive Tree Pruning by Physical Pretreatment. *Appl. Sci.* **2021**, *11*, 6445. [CrossRef]
16. Abdel-Halim, E.S.; Alanazi, H.H.; Al-Deyab, S.S. Utilization of Olive Tree Branch Cellulose in Synthesis of Hydroxypropyl Carboxymethyl Cellulose. *Carbohydr. Polym.* **2015**, *127*, 124–134. [CrossRef] [PubMed]
17. Callahan, A.M.; Dardick, C.; Scorza, R. Characterization of 'Stoneless': A Naturally Occurring, Partially Stoneless Plum Cultivar. *J. Am. Soc. Hortic. Sci.* **2009**, *134*, 120–125. [CrossRef]
18. Saeed, A.; Jahan, M.S.; Li, H.; Liu, Z.; Ni, Y.; van Heiningen, A. Mass Balances of Components Dissolved in the Pre-Hydrolysis Liquor of Kraft-Based Dissolving Pulp Production Process from Canadian Hardwoods. *Biomass Bioenergy* **2012**, *39*, 14–19. [CrossRef]
19. Garrote, G.; Domínguez, H.; Parajó, J.C. Autohydrolysis of Corncob: Study of Non-Isothermal Operation for Xylooligosaccharide Production. *J. Food Eng.* **2002**, *52*, 211–218. [CrossRef]
20. Li, H.; Saeed, A.; Jahan, M.S.; Ni, Y.; van Heiningen, A. Hemicellulose Removal from Hardwood Chips in the Pre-Hydrolysis Step of the Kraft-Based Dissolving Pulp Production Process. *J. Wood Chem. Technol.* **2010**, *30*, 48–60. [CrossRef]
21. Pérez-Armada, L.; Rivas, S.; González, B.; Moure, A. Extraction of Phenolic Compounds from Hazelnut Shells by Green Processes. *J. Food Eng.* **2019**, *255*, 1–8. [CrossRef]
22. Domingos, I.; Ferreira, M.; Ferreira, J.; Esteves, B. Olive Tree (*Olea europaea*) Pruning: Chemical Composition and Valorization of Wastes Through Liquefaction. *Sustainability* **2025**, *17*, 6739. [CrossRef]
23. *T 222 Om-02*; TAPPI Acid-Insoluble Lignin in Wood and Pulp. Test Method. TAPPI: Atlanta, GA, USA, 2002.
24. *T 429 Cm-10*; TAPPI Alpha-Cellulose in Paper, Test Method. TAPPI: Atlanta, GA, USA, 2010.

25. Cruz-Lopes, L.; Dulyanska, Y.; Domingos, I.; Ferreira, J.; Fragata, A.; Guiné, R.; Esteves, B. Influence of Pre-Hydrolysis on the Chemical Composition of Prunus Avium Cherry Seeds. *Agronomy* **2022**, *12*, 280. [CrossRef]
26. Romaní, A.; Garrote, G.; López, F.; Parajó, J.C. *Eucalyptus globulus* Wood Fractionation by Autohydrolysis and Organosolv Delignification. *Bioresour. Technol.* **2011**, *102*, 5896–5904. [CrossRef]
27. Cruz-Lopes, L.; Duarte, J.; Dulyanska, Y.; Guiné, R.P.; Esteves, B. Enhancing Liquefaction Efficiency: Exploring the Impact of Pre-Hydrolysis on Hazelnut Shell (*Corylus avellana* L.). *Materials* **2024**, *17*, 2667. [CrossRef] [PubMed]
28. Garrote, G.; Kabel, M.A.; Schols, H.A.; Falqué, E.; Domínguez, H.; Parajó, J.C. Effects of Eucalyptus Globulus Wood Autohydrolysis Conditions on the Reaction Products. *J. Agric. Food Chem.* **2007**, *55*, 9006–9013. [CrossRef]
29. Santos, T.M.; Alonso, M.V.; Oliet, M.; Domínguez, J.C.; Rigual, V.; Rodriguez, F. Effect of Autohydrolysis on *Pinus radiata* Wood for Hemicellulose Extraction. *Carbohydr. Polym.* **2018**, *194*, 285–293. [CrossRef]
30. Kyyrö, S.; Altgen, M.; Rautkari, L. Pressurized Hot Water Extraction of Scots Pine Sapwood: Effect of Wood Size on Obtained Treatment Products. *Biomass Conv. Bioref.* **2022**, *12*, 5019–5029. [CrossRef]
31. Torrado, I.; Dionísio, A.; Fernandes, M.C.; Roseiro, L.B.; Carvalheiro, F.; Pereira, H.; Duarte, L.C. Production of Oligosaccharides from Pine Nut Shells by Autohydrolysis. *Bioenerg. Res.* **2023**, *16*, 2253–2261. [CrossRef]
32. Amiri, H.; Karimi, K. Integration of Autohydrolysis and Organosolv Delignification for Efficient Acetone, Butanol, and Ethanol Production and Lignin Recovery. *Ind. Eng. Chem. Res.* **2016**, *55*, 4836–4845. [CrossRef]
33. Jia, W.; Shi, H.; Sheng, X.; Guo, Y.; Fatehi, P.; Niu, M. Correlation between Physicochemical Characteristics of Lignin Deposited on Autohydrolyzed Wood Chips and Their Cellulase Enzymatic Hydrolysis. *Bioresour. Technol.* **2022**, *350*, 126941. [CrossRef] [PubMed]
34. Jang, S.-K.; Jeong, H.; Choi, I.-G. The Effect of Cellulose Crystalline Structure Modification on Glucose Production from Chemical-Composition-Controlled Biomass. *Sustainability* **2023**, *15*, 5869. [CrossRef]
35. Yang, Q.; Chen, Y.; Yu, S.; Hou, Q.; Wu, M.; Jiang, T.; Wang, K.; Liu, W. Changes of Lignin Structure of Poplar Wood Chips in Autohydrolysis Pretreatment and Bleachability of Chemi-Thermomechanical Pulp. *Ind. Crops Prod.* **2022**, *176*, 114420. [CrossRef]
36. Lobato-Rodríguez, Á.; Gullón, B.; Garrote, G.; Del-Río, P.G. Enhancing *Acacia Dealbata* Valorization through Microwave-Assisted Autohydrolysis: An Energy-Efficient Approach to Oligosaccharides and Bioethanol Production. *Process Saf. Environ. Prot.* **2025**, *201*, 107470. [CrossRef]
37. Pérez-Pérez, A.; Gullón, B.; Lobato-Rodríguez, Á.; Garrote, G.; del Río, P.G. Microwave-Assisted Extraction of Hemicellulosic Oligosaccharides and Phenolics from *Robinia pseudoacacia* Wood. *Carbohydr. Polym.* **2023**, *301*, 120364. [CrossRef] [PubMed]
38. Michell, A.; Higgins, H. Infrared Spectroscopy in Australian Forest Products Research. In *Espectroscopia ATR-FTIR de Celulosa: Aspecto Instrumental y Tratamiento Matemático de Espectros*; CSIRO Forestry and Forest Products: St Lucia, QLD, Australia, 2002.
39. Coates, J.P. A Practical Approach to the Interpretation of Infrared Spectra. In *Encyclopedia of Analytical Chemistry*; John Wiley & Sons: Hoboken, NJ, USA, 2000; pp. 10815–10837.
40. Esteves, B.; Velez Marques, A.; Domingos, I.; Pereira, H. Chemical Changes of Heat Treated Pine and Eucalypt Wood Monitored by FTIR. *Maderas. Cienc. y Tecnol.* **2013**, *15*, 245–258. [CrossRef]
41. del Río, P.G.; Pérez-Pérez, A.; Garrote, G.; Gullón, B. Manufacturing of Hemicellulosic Oligosaccharides from Fast-Growing Paulownia Wood via Autohydrolysis: Microwave versus Conventional Heating. *Ind. Crops Prod.* **2022**, *187*, 115313. [CrossRef]
42. Dávila, I.; Gullón, P.; Labidi, J. Influence of the Heating Mechanism during the Aqueous Processing of Vine Shoots for the Obtaining of Hemicellulosic Oligosaccharides. *Waste Manag.* **2021**, *120*, 146–155. [CrossRef]
43. Ioelovich, M.J. Study of Thermal Energy of Alternative Solid Fuels. *Izvestiya vuzov. Appl. Chem. Biotechnol.* **2018**, *8*, 117–124. [CrossRef]
44. Esteves, B.; Sen, U.; Pereira, H. Influence of Chemical Composition on Heating Value of Biomass: A Review and Bibliometric Analysis. *Energies* **2023**, *16*, 4226. [CrossRef]
45. Demirbaş, A. Estimating of Structural Composition of Wood and Non-Wood Biomass Samples. *Energy Sources* **2005**, *27*, 761–767. [CrossRef]
46. Häggblom, P. The Potential of Lignin as a Maritime Biofuel. Master's Thesis, Laboratory of Process and Systems Engineering Faculty of Science and Engineering Åbo Akademi University, Turku, Finland, 2021.